2026 IEEE International Conference on Robotics and Automation (ICRA 2026)
June 1-5, 2026. Vienna, Austria

CareBot-H: Enhancing Patient Transfer with Biomimetic Design and Trajectory Deformation Algorithm

Deliang Zhu[1], Peizheng Li[2], Chunlei Meng[1], Jiexin Xie[3], Yang Li[2,*] and Shijie Guo[1,*]

***Abstract*—This paper introduces the CareBot-H Robot, a humanoid nursing robot designed to perform patient transfer tasks in confined environments. The robot is equipped with biomimetic arms that replicate human arm size and function, and distributed tactile sensors that enhance operational safety during physical contact. To achieve stable and humanoid motion, a trajectory deformation algorithm is proposed. The method comprises an offline phase, where expert demonstrations are encoded into prior trajectories using a Variational Autoencoder (VAE), and an online phase, where a tactile-informed Zero-Moment Point (ZMP) model enables real-time trajectory adjustment. Experimental validation with human participants demonstrates that the proposed approach outperforms manual teleoperation, producing smoother and more efficient transfer trajectories while significantly reducing deviations between actual and ideal ZMP. These results indicate that the CareBot-H achieves reliable and safe patient transfer performance, offering practical potential for deployment in real-world nursing care scenarios.**

I. Introduction

The accelerating growth of the aging population has intensified the demand for technological innovations in nursing care to ensure both efficiency and sustainability in elderly support [1], [2], [3]. Within this context, nursing robots have emerged as a promising solution, particularly for tasks that impose substantial physical strain on caregivers, such as patient transfers, dressing, and auxiliary mobility assistance [4]. Among these, patient transfer represents the most physically demanding operation, as it requires full-body handling of individuals with limited mobility. Beyond the sheer exertion, transfer tasks also involve highly dynamic human-robot interactions, where stability, safety, and precise force modulation are critical. These challenges underscore the need for nursing robots not only to provide sufficient lifting capacity but also to reproduce human-like motion strategies that ensure secure and reliable transfers in real-world care environments.

Significant progress has been achieved in the development of nursing robots for patient transfer, with systems such as C-Pam and Yanshan University's transfer platform demonstrating feasibility in real-world applications [5]. However, their bulky structures and limited maneuverability confine their use to spacious environments, restricting deployment in typical nursing scenarios. Humanoid robots, by contrast, are inherently better suited for environments tailored to human activity. Representative platforms such as RIBA [6] and RoNA [7] have been applied in compact nursing spaces, yet their rigid exteriors and insufficient sensing capabilities raise critical safety concerns, particularly in delicate patient-handling tasks. These limitations reveal a broader gap: existing robots lack both anthropomorphic motion consistency and robust sensory feedback to ensure safe physical interaction.

To address these challenges, this paper introduces the CareBot-H, a humanoid nursing robot equipped with biomimetic arms and distributed tactile sensing. The anthropomorphic mechanical arms are designed to replicate the dimensions and kinematics of human limbs, while the integrated tactile sensors enable fine-grained force monitoring during patient contact. Combined with a safety-oriented structural design, this configuration enhances interaction safety and provides a practical solution for patient transfer in confined care environments.

Exploring methods for humanoid nursing robots to replicate human actions during patient transfer tasks is crucial for enhancing their operational capabilities. Various strategies have been developed to enable these robots to adapt to complex and dynamic environments, improving both their effectiveness and safety in transfer tasks.

Replicating human motion in patient transfer tasks is fundamental to advancing the operational capability of humanoid nursing robots. Traditional control strategies, such as the artificial potential field method for obstacle avoidance [8], [9] and Zero-Moment Point (ZMP) techniques [10], [11], provide flexible mechanisms for dynamic adaptation. However, these approaches lack anthropomorphic consistency, as they typically optimize task execution without enforcing biomechanical constraints inherent to human movement. Consequently, robot trajectories may appear mechanically efficient yet kinematically unnatural, underscoring the necessity of incorporating implicit human motor principles that regulate joint coordination.

Compared to model-driven approaches, direct imitation of human demonstrations offers a more natural replication of human motion features. Among imitation-based strategies, teleoperation [12], [13], [14] provides a practical solution, allowing an experienced operator to act as an on-site physical proxy for the caregiver. This paradigm enables real-time trajectory adjustment to maintain patient balance in dynamic conditions. Nonetheless, reliance on visual perception alone often results in inadequate situational awareness [15], [16], which poses significant risks in safety-critical tasks such as

*This work was supported by the National Natural Science Foundation of China under Grant 52275018 and 2024 Shanghai Elderly Tech Support Program under Grant 4YL1900900.

[1]The authors are with College of Intelligent Robotics and Advanced Manufacturing, Fudan University, Shanghai 200433, China.

[2]The authors are with School of Mechanical Engineering, Hebei University of Technology, Tianjin 300401, China.

[3]The author is with School of Electronic Engineering and Automation, Guilin University of Electronic Technology, Guilin 541004, China.

*Shijie Guo and *Yang Li are co-corresponding authors. (email: guoshijie@fudan.edu.cn and liyang@hebut.edu.cn)

patient transfer. In contrast, tactile perception delivers continuous and fine-grained feedback of contact forces and interaction states, thereby compensating for the limitations of vision and ensuring reliable human-robot interaction.

To preserve anthropomorphic motion characteristics while ensuring real-time adaptability under continuous sensory feedback, this paper presents a trajectory deformation algorithm that integrates a tactile-informed ZMP stability model with operator expertise. The framework comprises two stages: offline training and online adaptation. In the offline stage, a task-representative dataset of teleoperated transfer demonstrations is used to train a Variational Autoencoder (VAE) [17]-[19], which captures latent representations of human coordination strategies and generates prior trajectories with anthropomorphic consistency. In the online stage, a distributed tactile-sensing-based stability model performs real-time corrective adaptation of these trajectories, maintaining balance and safety during patient transfer. By coupling prior human-inspired trajectories with tactile feedback-driven stability control, the proposed algorithm simultaneously achieves anthropomorphic consistency and dynamic stability, thereby addressing critical limitations of conventional imitation and model-based approaches.

The main contributions can be summarized as follows:

1) The CareBot-H is introduced with biomimetic arms replicating human limb size and kinematics, enabling safe and effective transfers in confined environments.
2) A trajectory deformation algorithm is proposed, which integrates VAE-based expert priors with a tactile-informed ZMP stability model to ensure real-time, anthropomorphic, and stable motion adaptation.
3) The proposed framework is experimentally validated, demonstrating significant improvements in safety, efficiency, and ZMP tracking accuracy during patient transfer, as illustrated in Fig. 1.

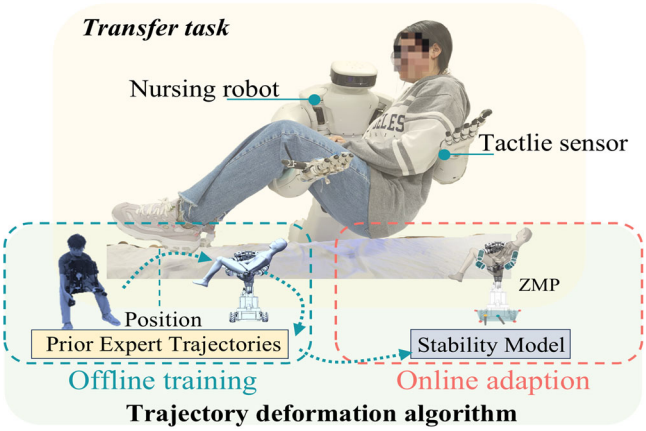

Fig. 1. The Overview of the CareBot-H and the Trajectory Deformation Algorithm for Patient Transfer Tasks.

II. Humanoid Nursing CareBot-H

A. CareBot-H

The CareBot-H is designed as a humanoid nursing platform to address demanding care tasks such as patient transfer, mobility assistance, and fluid handling. Its mechanical architecture integrates an anthropomorphic dual-arm system with a rotatable and bendable waist, enabling the robot to reproduce human-like movements for precise and safe nursing operations. The system supports a total payload of 105 kg, with each arm capable of lifting 45 kg at the end effector and achieving a maximum joint angular velocity of 37.5°/s, ensuring sufficient strength and responsiveness for patient handling in confined environments.

As illustrated in Fig. 2, the CareBot-H consists of six functional modules: a mobile chassis, waist, shoulders, elbows, hands, and distributed tactile sensors [20], [21]. The waist employs a combination of a high-reduction-ratio harmonic drive and worm gear transmission to enhance stability and load-bearing capability. The mobile chassis, equipped with Mecanum wheels, provides omnidirectional mobility in restricted clinical spaces. To ensure safe physical interaction, flexible tactile sensors are embedded along the arms and chest, offering fine-grained perception of contact forces during human-robot interaction.

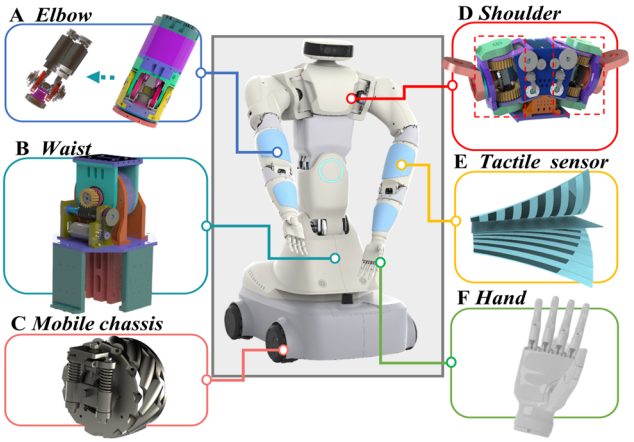

Fig. 2. The Structural Components of the CareBot-H.

B. Anthropomorphic Arm

The anthropomorphic arms are designed with biomechanical consistency, featuring modular construction, integrated sensing, and high torque output. While humanoid arms typically require high degrees of freedom (DOF) to replicate natural human motion, independent actuation of each DOF often increases actuator count, wiring complexity, and structural bulk, compromising smoothness and compactness. To address this challenge, a coupled-drive joint technology is introduced (Fig. 3). Using differential coupling and an optimized transmission chain, two motors are synchronized to actuate two DOF, eliminating the need for vertical placement. Bevel gears further coordinate motion across both DOF, ensuring structural compactness, morphological continuity, and efficient actuation. For modularization, each joint is divided into electrical and mechanical units connected seamlessly, resembling the continuity of human vessels. This design facilitates scalable assembly and preserves a cohesive external morphology across modules.

High torque delivery is achieved through a dual-motor drive system that balances torque and speed. Multi-stage reductions via timing belt pulleys, harmonic reducers, and hypoid gears yield an optimized ratio of 3060:1, enabling sufficient output torque for safe execution of heavy-load transfer tasks. Compared with representative humanoid

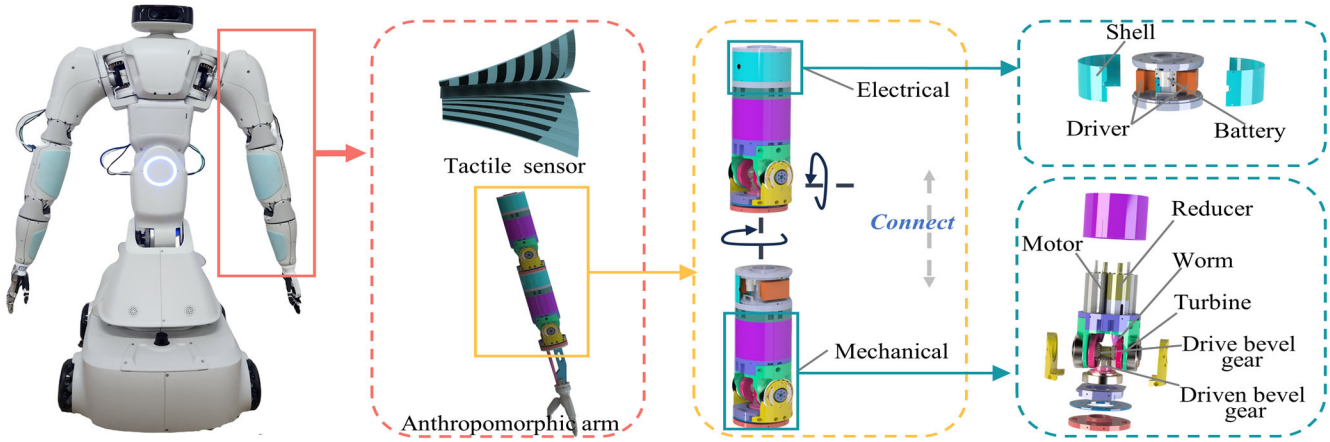

Fig. 3. Structure of the CareBot-H's anthropomorphic arm, showing integrated tactile sensors, and modular electrical and mechanical units.

robots such as Ambidex [22], Fourier, Unitree [23], and HRP-4c [24], the CareBot-H demonstrates distinct advantages. Its arm length of 850 mm surpasses the 500-700 mm range of existing platforms, expanding the operational workspace, while its torque-to-weight ratio of 143.595 N·m/kg is the highest among humanoid arms of similar size. These characteristics establish the CareBot-H as a uniquely capable platform for safe, high-capacity patient transfer in confined nursing environments.

C. Biomimetic Sensing

The biomimetic design of the arm further incorporates integrated tactile sensing. The tactile sensing system consists of a capacitive array sensor and a DAQ board for real-time acquisition of capacitive signals. Each sensor unit is composed of a protective membrane, a compressible dielectric elastomer layer, and electrode layers fabricated from conductive tape or ion-coated films. A 32×32 capacitor matrix, formed by orthogonally arranged electrodes, enables high-resolution pressure mapping across the arm surface. The sensing mechanism relies on monitoring capacitance variations induced by the deformation of the dielectric layer under applied pressure, thereby providing quantitative measurements of distributed contact forces. This design offers fine-grained tactile feedback essential for ensuring safe and compliant human-robot interaction during patient handling.

III. Trajectory Deformation Algorithm

To ensure dynamic stability and operational safety during patient transfer, this study proposes a trajectory deformation-based motion regulation algorithm. The overall framework consists of two components: an offline stage for expert-prior learning and an online stage for tactile-informed adaptation, as shown in Fig. 4.

In the offline stage, teleoperated demonstrations of transfer tasks are used to train a VAE, which learns the latent distribution of expert motions and generates prior trajectories. These priors preserve anthropomorphic kinematic coordination and ergonomic plausibility while filtering out posture deviations induced by environmental disturbances, thereby providing a reliable reference distribution for subsequent real-time regulation.

In the online stage, a stability model that integrates tactile sensing with the Zero-Moment Point (ZMP) criterion is employed to continuously refine the prior trajectories. By leveraging distributed tactile signals, the model monitors and regulates human-robot interaction forces in real time, preventing patient imbalance or instability. Ultimately, the algorithm achieves stability-constrained anthropomorphic trajectory generation, ensuring safe and reliable execution of patient transfer tasks in complex nursing environments.

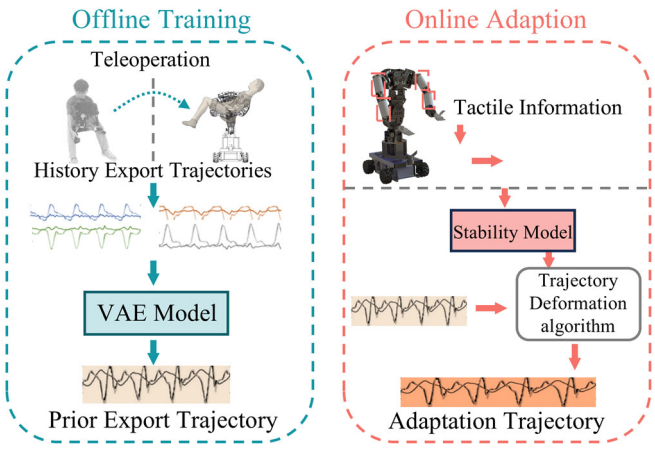

Fig. 4. Framework of the trajectory deformation algorithm, consisting of offline VAE-based prior trajectory generation and online tactile-feedback adaptation.

A. Prior expert trajectories

To establish an initial reference trajectory for patient transfer tasks, expert demonstrations were collected using a custom teleoperation system. The master device is a bionic dual-arm operation platform with 14 degrees of freedom, actuated by high-torque motors. Its dimensions are ergonomically scaled to two-thirds of the nursing robot's arms, ensuring usability while preserving anthropomorphic joint mapping. The operator's motions are transferred through joint-level position control, where the measured joint angles and velocities of the master device are directly mapped to the corresponding joints of the nursing robot via forward kinematics.

During teleoperation, the following data streams were recorded at a frequency of 100 Hz:

1) Joint angles
2) Joint velocities
3) End-effector Cartesian positions and orientations.

These kinematic data provide sufficient information to characterize the expert's motion during transfer tasks.

All recorded trajectories were resampled to a fixed length via cubic spline interpolation and normalized to zero mean and unit variance. This preprocessing step ensured consistency across demonstrations and facilitated model training.

A VAE was then applied to capture the statistical distribution of the expert trajectories and to generate coarse prior trajectories that encode human-like joint coordination. The VAE adopts a stacked LSTM encoder-decoder architecture to model the temporal evolution of trajectories. The encoder consists of two LSTM layers (128 hidden units each), compressing sequential motion data into a 4-dimensional latent vector by estimating its mean and variance. The decoder mirrors this structure and reconstructs the trajectories in the 14-dimensional joint space of the nursing robot.

The training objective combines reconstruction accuracy and latent regularization:

$$\mathcal{L} = \mathcal{L}_{rec} + \beta D_{KL}(q(z \mid x) \| p(z)) \tag{1}$$

where $\mathcal{L}_{\text{rec}}$ is the mean squared error between the reconstructed and original trajectories, and D_{KL} is the Kullback-Leibler divergence. The balance coefficient was set to $\beta = 0.01$. Training was performed using the Adam optimizer (learning rate 1e-3, batch size 64) for 200 epochs on an NVIDIA RTX 3090 GPU, with a total runtime of approximately 4 hours. Generated trajectories were further smoothed using a low-pass filter to eliminate high-frequency fluctuations.

Importantly, the VAE is not designed to replicate expert demonstrations verbatim. Instead, it learns a compact representation of expert transfer strategies and produces a coarse, human-like prior trajectory that captures general movement patterns. This trajectory serves as a data-driven baseline, which is further refined online by the tactile-feedback-based stability model to adapt to patient-specific conditions and ensure safety.

B. Online Tactile-Informed Adaptation (ZMP Model)

Building upon offline-generated trajectories, the proposed stability model integrates distributed tactile feedback with the ZMP criterion to guarantee dynamic equilibrium during patient transfer tasks executed by the CareBot-H. The ZMP framework, widely adopted as a fundamental metric of dynamic stability, defines the equilibrium point on the support plane at which the resultant moment of all external forces has no horizontal component. In the context of nursing transfer, the emphasis on ground-perpendicular moments is motivated by the fact that the predominant hazard to patient safety is lateral tipping or overturning, which is primarily induced by horizontal moment components. Constraining these components to zero therefore provides a rigorous stability condition for maintaining balance during transfer. As long as the computed ZMP remains strictly within the support polygon, the system preserves stability and prevents destabilization. Unlike bipedal robots, where the support region is determined by foot-ground contacts, in patient transfer scenarios it is defined by the distributed arm-patient contact interfaces. These interfaces simultaneously provide essential load-bearing support and introduce perturbation-sensitive interaction dynamics, rendering real-time ZMP estimation and trajectory modulation indispensable for safe execution.

To enable stability estimation under human-robot contact, distributed tactile sensors embedded along the robot arms are employed to measure local normal forces at interaction points. For the i-th contact point in the base coordinate system $\mathcal{F}_O = \{O; x_O, y_O, z_O\}$ with position $\mathbf{r}_i = [x_i, y_i, z_i]^T$. the tactile sensor outputs a calibrated normal force magnitude $f_i^{(n)}$. The corresponding force vector is expressed as $\mathbf{f}_i = f_i^{(n)} \mathbf{n}_i$ where $\mathbf{n}_i$ is the unit normal direction in the global frame. The total contact force and the resultant moment about the base origin O are given by

$$\mathbf{F} = \sum_{i=1}^{N} \mathbf{f}_i, \mathbf{M}^O = \sum_{i=1}^{N} \mathbf{r}_i \times \mathbf{f}_i. \tag{2}$$

Under quasi-static conditions, the rate of angular momentum can be neglected. The ZMP coordinates on the support plane $\Pi : z_O = 0$ are then

$$x_{\text{zmp}} = -\frac{M_y^O}{F_z}, y_{\text{zmp}} = \frac{M_x^O}{F_z} \tag{3}$$

where $F_z = \mathbf{F} \cdot \mathbf{e}_z$ denotes the vertical resultant force.

The support polygon is defined by projecting all valid contact points(with $f_i^{(n)} > \tau$)onto the ground plane, with the convex hull forming the polygon PPP. According to Eq. (3), system stability is preserved when the computed ZMP coordinates $(x_{\text{zmp}}, y_{\text{zmp}})$ remain within the interior of P. Once the ZMP deviates from its reference value (x_{zmp}^d, y_{zmp}^d), the deviation $\Delta P_{zmp}$is interpreted as a stability error signal.

To establish the physical intuition behind the corrective control, the mapping between the ZMP coordinates and the supporting contact links must first be clarified. A deviation in the ZMP position, for instance along the x-axis, indicates that the resultant moment about the support surface is unbalanced in that direction. In practical terms, this requires a compensatory adjustment of the end-effector or supporting links so that the net contact force distribution shifts accordingly to re-center the ZMP within the support polygon. Similarly, deviations along the y-axis are corrected by coordinated adjustments of the relevant links in the sagittal plane.

Rather than applying this compensation directly in joint space, the deviation of the ZMP from its reference is first reformulated as an equivalent corrective force or acceleration in Cartesian space. This step provides an intuitive representation: a shift of the ZMP corresponds to a virtual restoring force that "pulls" the robot's end-effector configuration back toward balance. The corrective Cartesian

acceleration derived in this manner is then mapped into the joint space through the Jacobian matrix and its time derivative, which provide the kinematic relationship between end-effector motions and joint accelerations. In effect, the Jacobian ensures that a corrective displacement of the ZMP along the support plane is translated into coordinated adjustments of multiple joints.

Finally, the resulting corrective joint accelerations are superimposed on the nominal joint commands generated from the VAE-based prior trajectories. This superposition preserves the anthropomorphic coordination patterns embedded in the prior while dynamically adjusting the motion to maintain stability. Through this formulation, the corrective action is grounded in a clear physical relationship-ZMP deviations dictate how supporting links must be reconfigured-while the mathematical mapping ensures that these corrections are consistently integrated into the robot's overall motion plan.

Through this closed-loop process, ZMP deviations are rigorously embedded into the robot's kinematic and dynamic control chain: starting from contact force measurements on the support plane, they are translated into virtual forces, converted via the Jacobian into joint-level corrections, and finally integrated into the trajectory execution. This mechanism ensures that the robot continuously realigns its motion to drive the ZMP back inside the support polygon, thereby achieving dynamic stability while preserving anthropomorphic motion and patient comfort during transfer.

Since trajectories generated by the VAE originate from a general demonstration dataset, they capture diverse but non-personalized motion patterns. To enhance patient-specific adaptability, the stability model refines these trajectories online, compensating for individual variations while preserving anthropomorphic postures. With two eight-degree-of-freedom arms (six in each arm and two in the waist), the system flexibly resolves redundancy in end-effector poses, enabling stable and reliable execution of transfer tasks.

Therefore, the optimization objective of the proposed algorithm is to simultaneously regulate ZMP motion and enforce end-effector pose tracking while executing the prior trajectories, thereby achieving a balance between stability and trajectory preservation. Specifically, ZMP deviations provide the constraint for dynamic stability, whereas the end-effector poses encode the anthropomorphic consistency derived from expert demonstrations. By establishing a coupled optimization relationship between these two objectives, the algorithm ensures patient safety while maintaining human-like motion characteristics and smooth task execution.

To simultaneously enforce ZMP tracking and adherence to the expert prior trajectories, deviations between the planned and actual poses are characterized using forward kinematics and the Jacobian, yielding the reference pose trajectory $\{\boldsymbol{p}_t^d, \dot{\boldsymbol{p}}_t^d\}_{t=0}^T$. The reference pose velocity derived from the impedance relationship is expressed as

$$\dot{\boldsymbol{p}}_t^c = \dot{\boldsymbol{p}}_t^c + \dot{\boldsymbol{p}}_t^I \tag{4}$$

However, corrections induced by the ideal ZMP through joints 3 and 5 inevitably cause deviations in the end-effector pose. To account for this, the difference between the actual pose and the planned pose is represented not by direct addition, but through rotation matrices that avoid singularities such as gimbal lock:

$$\boldsymbol{p}_t^c \neq \boldsymbol{p}_t^d + \boldsymbol{p}_t^I \tag{5}$$

Although the description of attitude angles is not unique, the corresponding rotation matrix remains the same. Therefore, we use the rotation matrix to describe the differences in pose. The attitude angles represent rotations around the fixed z, y, x axes by γ, β, α respectively. The corresponding rotation matrix is:

$$\begin{aligned}\boldsymbol{R} &= \boldsymbol{R}_{z,\gamma}\boldsymbol{R}_{y,\beta}\boldsymbol{R}_{x,\alpha} \\ &= \begin{bmatrix} c\beta c\gamma & -c\beta s\gamma + s\alpha s\beta c\gamma & s\alpha s\gamma + c\alpha s\beta c\gamma \\ c\beta s\gamma & c\alpha c\gamma + s\alpha s\beta s\gamma & -s\alpha c\gamma + c\alpha s\beta s\gamma \\ -s\beta & s\alpha c\beta & c\alpha c\beta \end{bmatrix}\end{aligned} \tag{6}$$

The homogeneous transformation matrix of the reference pose p^c relative to the base coordinate system is given by:

$$\begin{aligned}\boldsymbol{T}_c^O &= \boldsymbol{T}(\boldsymbol{p}^d)\boldsymbol{T}(\boldsymbol{p}^I) \\ &= \begin{bmatrix} \boldsymbol{R}_d^O\boldsymbol{R}_I^O & (\boldsymbol{X}_d^O + \boldsymbol{X}_I^O)^{\mathrm{T}} \\ \boldsymbol{0}^{1\times 3} & 1 \end{bmatrix}\end{aligned} \tag{7}$$

The rotation matrix of the reference pose relative to the current pose $\boldsymbol{p}^p$ is given by:

$$\boldsymbol{T}_c^p = (\boldsymbol{T}_p^o)^{-1}\boldsymbol{T}_c^o \tag{8}$$

The rotation matrix $\boldsymbol{R}_c^p$ can be converted to the attitude angles $\boldsymbol{W}_c^p$:

$$\boldsymbol{W}_c^p = \begin{bmatrix} \mathrm{Atan}\left(\frac{\boldsymbol{R}_{c,32}^p}{c\beta^c}, \frac{\boldsymbol{R}_{c,33}^p}{c\beta^c}\right) \\ \mathrm{Atan2}\left(-\boldsymbol{R}_{c,31}^p, \sqrt{\left(\boldsymbol{R}_{c,11}^p\right)^2 + \left(\boldsymbol{R}_{c,21}^p\right)^2}\right) \\ \mathrm{Atan2}\left(\frac{\boldsymbol{R}_{c,21}^p}{c\beta^c}, \frac{\boldsymbol{R}_{c,11}^p}{c\beta^c}\right) \end{bmatrix}^{\mathrm{T}} \tag{9}$$

The difference between the actual end-effector pose of the robotic arm and the planned pose at any given moment in the current coordinate system $\boldsymbol{R}_p^O$ is given by:

$$d_p(\boldsymbol{p}^c, \boldsymbol{p}^p) = \mathrm{vec}\{[\boldsymbol{X}_c^p, \boldsymbol{W}_c^p]\}^{\mathrm{T}} \tag{10}$$

Namely the end-effector of the robotic arm moves along the current coordinate system R_p^O by $\boldsymbol{X}_c^p$ and then rotates around the current coordinate system R_p^O by $\boldsymbol{W}_c^p$. To convert the pose velocity into joint velocity, it is necessary to calculate the mapping of $d_p(\boldsymbol{p}^c, \boldsymbol{p}^p)$ in the base coordinate system.

$$d(\boldsymbol{p}^c, \boldsymbol{p}^p) = \mathrm{vec}\{[\boldsymbol{R}_p^O\boldsymbol{X}_c^p, \boldsymbol{R}_p^O\boldsymbol{W}_c^p]\}^{\mathrm{T}} \tag{11}$$

When the CareBot-H transfers the patient, smooth and gentle movements are crucial. Therefore, a gravitational potential energy based on the pose difference is established. This gravitational approach applies the target-following task within an acceleration field:

$$U_a(\boldsymbol{p}) = \frac{1}{2}\eta_a \|d(\boldsymbol{p}^c, \boldsymbol{p}^p)\|^2 \tag{12}$$

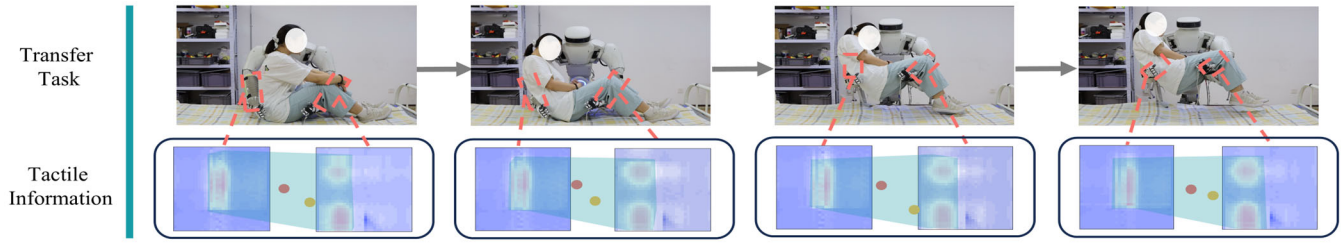

(a) Tactile Feedback and ZMP Variations based on Teleoperation in Transfer Tasks

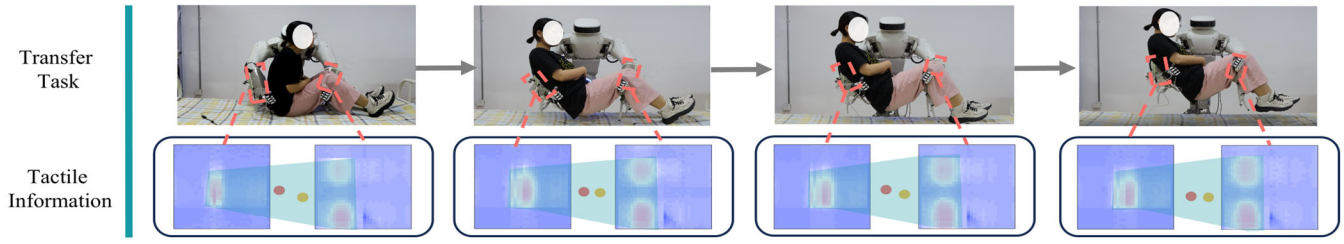

(b) Tactile Feedback and ZMP Variations Based on Trajectory Deformation Algorithms in Transfer Tasks

Fig. 5. Comparison of tactile feedback and ZMP variations during patient transfer tasks. (a) Teleoperation shows larger fluctuations in tactile interaction and ZMP deviation. (b) The proposed trajectory deformation algorithm yields smoother tactile feedback and reduced ZMP deviation, ensuring more stable and safe transfers.

In the (9), η_a is the gravitational field gain. The gradient of the gravitational potential energy with respect to the pose deviation $d(\boldsymbol{p}^c, \boldsymbol{p}^p)$ represents the gravitational force:

$$f^a = \nabla_{d(p^c,p^p)} U_a(\boldsymbol{p}) = \eta_a d(\boldsymbol{p}^c, \boldsymbol{p}^p) \tag{13}$$

Assuming the virtual positive definite inertia matrix at the end-effector is $\boldsymbol{M}_{ob} \in \mathbb{R}^{6\times6}$:

$$\ddot{\boldsymbol{p}}^p = \boldsymbol{M}_{ob}^{-1} \begin{bmatrix} f^a \\ \boldsymbol{0}^{3\times1} \end{bmatrix} \tag{14}$$

By using the Jacobian matrix, the pose acceleration can be transformed into the joint space. The relationship between the end-effector's pose acceleration and the joint acceleration is given by:

$$\ddot{\boldsymbol{q}}^a = \delta\left(\boldsymbol{J}^{-1}\ddot{\boldsymbol{p}}^p - \boldsymbol{J}^{-1}\dot{\boldsymbol{J}}\dot{\boldsymbol{p}}^p\right) \tag{15}$$

In this equation, δ is a gain coefficient used to adjust the mapping of the repulsive force in the joint space.

Thus, the angular trajectory deviation at any given moment is:

$$\begin{cases} \boldsymbol{q}_{t+1}^o = \boldsymbol{q}_{t+1}^o + \dot{\boldsymbol{q}}_{t+1}^o dt \\ \dot{\boldsymbol{q}}_{t+1}^o = \dot{\boldsymbol{q}}_t^o + \ddot{\boldsymbol{q}}_{t+1}^o dt \\ \ddot{\boldsymbol{q}}_{t+1}^o = \ddot{\boldsymbol{q}}_t^o + \ddot{\boldsymbol{q}}_t^a + \ddot{\boldsymbol{q}}_t^e \end{cases} \tag{16}$$

IV. Experiments

To validate the effectiveness of the proposed trajectory deformation algorithm, comparative experiments were conducted between teleoperation and the algorithm-based control during patient transfer tasks. Ten participants with varying physical conditions were recruited, and transfer trials were performed under two conditions: (i) manual teleoperation executed by an experienced operator (over 20 hours of training), and (ii) the proposed trajectory deformation algorithm. Each participant completed five trials per condition, resulting in a total of 100 transfer experiments.

Before presenting the results, the calibration of the ideal and actual ZMP used in this study is illustrated in Fig. 6. This diagram defines the reference framework for stability assessment, where deviations between the actual ZMP and the ideal ZMP are used as a key performance metric throughout the experiments.

A. Prior Expert Trajectories

Among the 100 transfer trials, 20 optimal demonstrations (two per participant) were selected to construct prior expert trajectories, with optimality determined by post-task questionnaires assessing perceived tipping risk and comfort.

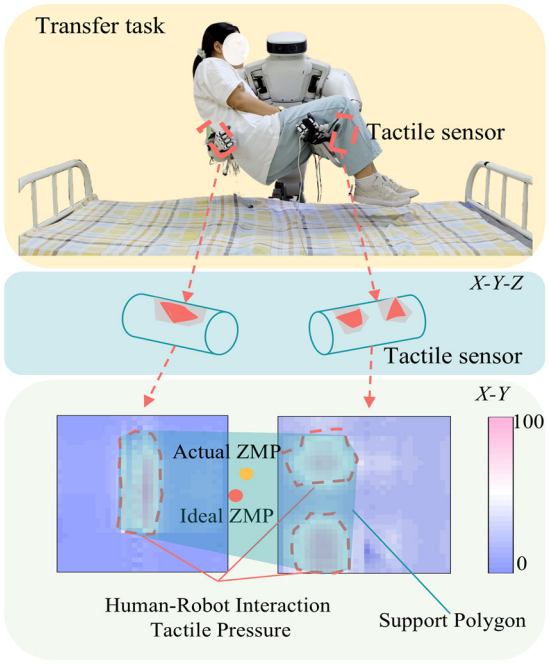

Fig. 6. Calibration of the ideal and actual Zero-Moment Point (ZMP) used as the stability reference in patient transfer tasks.

These trajectories were used to train a VAE with a stacked LSTM encoder-decoder and a latent space dimension of 4. The VAE successfully captured the statistical distribution of demonstrations and generated prior trajectories that preserved anthropomorphic coordination patterns. Fig. 7 shows representative prior trajectories, confirming their consistency and ergonomic suitability for transfer tasks.

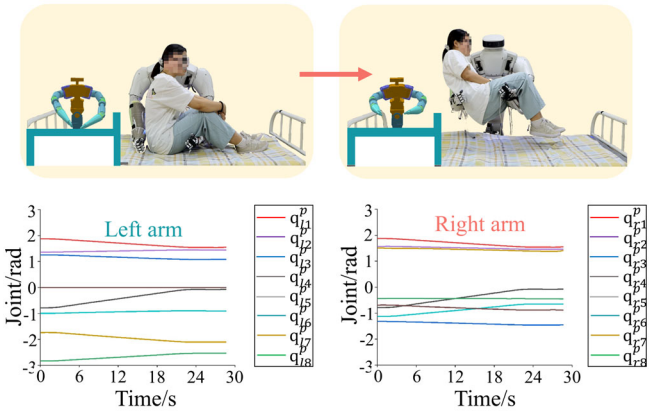

Fig. 7. Representative prior expert trajectories generated by the Variational Autoencoder from teleoperated demonstrations, preserving anthropomorphic coordination patterns.

B. Evaluation of Trajectory Deformation Algorithm

The algorithm was then evaluated against teleoperation using the same group of participants to ensure consistency and comparability of results. As illustrated in Fig. 5, the actual ZMP obtained during manual teleoperation showed substantial fluctuations and frequent deviations from the ideal reference. Such deviations can be attributed to limited operator visibility, hand tremors, and delayed corrective actions, all of which reduce the reliability of stability control in safety-critical tasks. In contrast, the trajectory deformation algorithm consistently maintained closer alignment with the ideal ZMP, demonstrating its ability to compensate for perturbations and preserve balance throughout the transfer. This finding highlights the algorithm's advantage in dynamically stabilizing human-robot interactions where minor instabilities can pose significant risks.

Fig. 8(a)-(b) provides a direct comparison of transfer trajectories under the two conditions. Teleoperated transfers produced irregular, non-smooth paths, often elongated due to repeated corrective motions. By contrast, the algorithm generated trajectories that were not only smoother but also shorter in duration, reflecting both higher motion efficiency and reduced physical stress on the patient. These results suggest that the deformation algorithm can simultaneously improve the safety of physical interaction and enhance the overall task efficiency, a combination particularly critical in real-world nursing environments where caregivers must perform frequent transfers.

To further quantify these improvements, the mean squared error (MSE) between the actual and ideal ZMP was calculated as an objective stability metric. Fig. 8(c) shows representative MSE curves for teleoperation and algorithm-based trials. The algorithm consistently achieved lower error across the entire transfer process, whereas teleoperation trials showed larger oscillations and higher error peaks. Across all participants, the average MSE was reduced by 54% compared to teleoperation, and the improvement was statistically significant ($p < 0.05$, paired t-test). This reduction in ZMP tracking error provides quantitative confirmation that the proposed trajectory deformation algorithm enhances dynamic stability and ensures safer patient handling during transfer tasks.

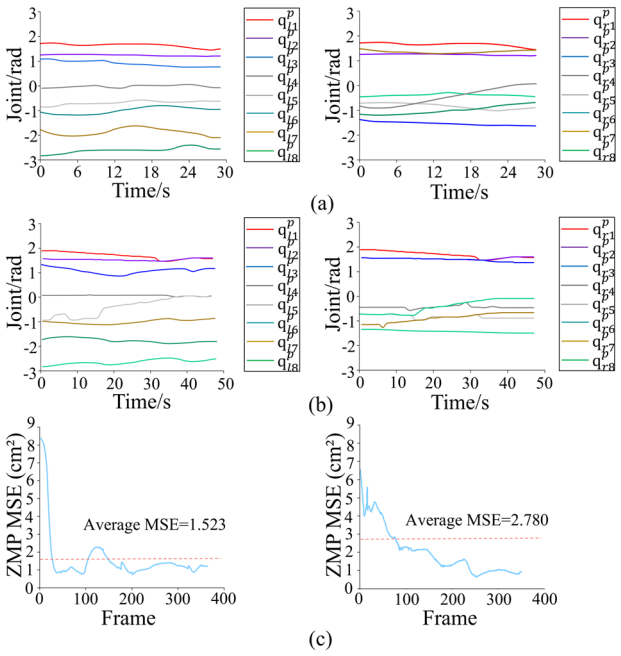

Fig. 8. Comparative evaluation of teleoperation and the proposed trajectory deformation algorithm during patient transfer tasks: (a) Transfer trajectory obtained through manual teleoperation, showing irregularities and tremor-induced deviations; (b) Transfer trajectory generated by the proposed algorithm, producing smoother and shorter-duration paths; (c) Real-time mean squared error (MSE) between actual and ideal ZMP: the left figure shows the proposed trajectory deformation algorithm, yielding consistently lower error; the right figure shows manual teleoperation, with larger fluctuations and higher deviations.

V. Conclusion

This paper presented CareBot-H, a humanoid nursing robot equipped with biomimetic arms and tactile sensors for patient transfer in confined spaces. A trajectory deformation algorithm was proposed, integrating VAE-based expert priors with tactile-informed ZMP regulation. Experimental results demonstrated that the algorithm outperformed manual teleoperation by producing smoother, safer, and more efficient trajectories.

The study is limited by a relatively small participant sample, which constrains the generalizability of the findings. Future work will expand the evaluation scale and conduct clinical validation in real-world environments. In addition, subsequent research will explore multimodal sensory integration and personalized adaptive control to further enhance robustness and clinical applicability.

References

[1] K. Wada, T. Shibata, T. Saito and K. Tanie, "Effects of robot-assisted activity for elderly people and nurses at a day service center," Proceedings of the IEEE, vol. 92, no. 11, pp. 1780-1788, Nov. 2004.

[2] G. Yang et al., "Homecare Robotic Systems for Healthcare 4.0: Visions and Enabling Technologies, " *IEEE Journal of Biomedical and Health Informatics*, vol. 24, no. 9, pp. 2535-2549, Sept. 2020.

[3] M. Nasr, M. M. Islam, S. Shehata, F. Karray and Y. Quintana, "Smart Healthcare in the Age of AI: Recent Advances, Challenges, and Future Prospects, " *IEEE Access,* vol. 9, pp. 145248-145270, 2021.

[4] K. Darvish et al., "Teleoperation of Humanoid Robots: A Survey, " *IEEE Transactions on Robotics*, vol. 39, no. 3, pp. 1706-1727, June 2023.

[5] G. Chen et al. "An overview of transfer nursing robot: Classification, key technology, and trend," *Robotics and Autonomous Systems*, vol. 174, April 2024.

[6] T. Mukai et al., "Development of a nursing-care assistant robot RIBA that can lift a human in its arms," in *2010 IEEE/RSJ International Conference on Intelligent Robots and Systems*, Taipei, Taiwan, 2010, pp. 5996-6001.

[7] J. Ding et al., "Giving patients a lift - the robotic nursing assistant (RoNA), " in *2014 IEEE International Conference on Technologies for Practical Robot Applications (TePRA)*, Woburn, MA, USA, 2014, pp. 1-5.

[8] B. Zhang, S. Hu and Q. Wang, "A Head Posture-based Interactive Method of Auxiliary Mobile Robot for Direction Recognition and Obstacle Avoidance, " in 2*023 5th International Academic Exchange Conference on Science and Technology Innovation (IAECST),* Guangzhou, China, 2023, pp. 1540-1545.

[9] I. Iancu and B. Iancu, "Designing mobile technology for elderly. A theoretical overview, " *Technological Forecasting and Social Change*, vol. 155, 2020.

[10] P. Di, J. Huang, S. Nakagawa, K. Sekiyama and T. Fukuda, "Fall detection and prevention in the elderly based on the ZMP stability control, " in *2013 IEEE Workshop on Advanced Robotics and its Social Impacts*, Tokyo, Japan, 2013, pp. 82-87.

[11] P. Di, J. Huang, S. Nakagawa, K. Sekiyama and T. Fukuda, "Fall detection for the elderly using a cane robot based on ZMP estimation, " in *MHS2013*, Nagoya, Japan, 2013, pp. 1-6.

[12] R. K. Megalingam, S. K. Manoharan and A. H. Kota, "Annapoorna – Food, Water and Medicine Delivery Teleoperated Robot with Telemedicine Facility," in *2024 International Conference on E-mobility, Power Control and Smart Systems (ICEMPS)*, Thiruvananthapuram, India, 2024, pp. 1-6.

[13] H. Su, J. Sandoval, M. Makhdoomi, G. Ferrigno and E. De Momi, "Safety-Enhanced Human-Robot Interaction Control of Redundant Robot for Teleoperated Minimally Invasive Surgery, " in *2018 IEEE International Conference on Robotics and Automation (ICRA)*, Brisbane, QLD, Australia, 2018, pp. 6611-6616.

[14] J. Xie, D. Zhu, J. Wang and S. Guo, "A Training-Evaluation Method for Nursing Telerobot Operator with Unsupervised Trajectory Segmentation," in *2022 IEEE/RSJ International Conference on Intelligent Robots and Systems (IROS)*, Kyoto, Japan, 2022, pp. 1848-1854.

[15] P. Huang, Y. Ishibashi and M. Sithu, "Enhancement of simultaneous output-timing control with human perception of synchronization errors among multiple destinations," in *2016 2nd IEEE International Conference on Computer and Communications (ICCC)*, Chengdu, China, 2016, pp. 2099-2103.

[16] X. Zhang, "Control Technology of Terminal Attitude Adjustment of Traction Parallel Robot Based on Visual Perception," in *2021 IEEE 2nd International Conference on Big Data, Artificial Intelligence and Internet of Things Engineering (ICBAIE)*, Nanchang, China, 2021, pp. 1045-1049.

[17] A. Abe, G. Pongthanisorn, S. -i. Kaneko and G. Capi, "Enhancing Robot Self-Localization Accuracy and Robustness: A Variational Autoencoder-Based Approach, " in *2023 5th International Conference on Control and Robotics (ICCR)*, Tokyo, Japan, 2023, pp. 145-149.

[18] V. Prasad, D. Koert, R. Stock-Homburg, J. Peters and G. Chalvatzaki, "MILD: Multimodal Interactive Latent Dynamics for Learning Human-Robot Interaction," in *2022 IEEE-RAS 21st International Conference on Humanoid Robots (Humanoids)*, Ginowan, Japan, 2022, pp. 472-479.

[19] V. Prasad, A. Kshirsagar, D. Koert, R. Stock-Homburg, J. Peters and G. Chalvatzaki, "MoVEInt: Mixture of Variational Experts for Learning Human–Robot Interactions From Demonstrations," *IEEE Robotics and Automation Letters*, vol. 9, no. 7, pp. 6043-6050, July 2024.

[20] F. Hou, J. Liu, K. Liu, P. Wang, G. Li and S. Guo, "3-D-Curved Iontronic Tactile Sensor and Denoising Method for Physical Human–Robot Interactions, " *IEEE Sensors Journal*, vol. 23, no. 7, pp. 7667-7682, 1 April, 2023.

[21] Q. Tian, J. Liu, K. Liu and S. Guo, "Tactile Features of Human Finger Contact Motor Primitives," *IEEE Transactions on Haptics*, vol. 16, no. 4, pp. 848-860, 2023.

[22] Y. -J. Kim, J. -I. Kim and W. Jang, "Quaternion Joint: Dexterous 3-DOF Joint Representing Quaternion Motion for High-Speed Safe Interaction," in *2018 IEEE/RSJ International Conference on Intelligent Robots and Systems (IROS)*, Madrid, Spain, 2018, pp. 935-942.

[23] C. Zhang, W. Xiao, "WoCoCo: Learning Whole-Body Humanoid Control with Sequential Contacts," *arXiv preprintarXiv*: 2406.06005v1, 2024.

[24] K. Kaneko, F. Kanehiro, M. Morisawa, K. Miura, S. Nakaoka and S. Kajita, "Cybernetic human HRP-4C," in *2009 9th IEEE-RAS International Conference on Humanoid Robots*, Paris, France, 2009, pp. 7-14.

[25] K. Mitobe and G. Capi, "A global stability analysis of legged balance controllers under ZMP constraints," in *2023 IEEE International Symposium on Robotic and Sensors Environments (ROSE)*, Tokyo, Japan, 2023, pp. 1-6.

[26] B. Xing, Y. Liu, Z. Wang, J. Zhao, T. Qiu and T. Yan, "Dynamic Walking Locomotion Framework Based on Impulse Force Design and ZMP Principle," in *2022 34th Chinese Control and Decision Conference (CCDC)*, Hefei, China, 2022, pp. 1995-2000.